Aerospace Science and Technology 153 (2024) 109419

Contents lists available at ScienceDirect

Aerospace Science and Technology

journal homepage: www.elsevier.com/locate/aescte

Reduced-order helicopter model identification from closed-loop data

Claudio Pasquali [a], Jacopo Serafini [a], Massimo Gennaretti [a,*], Riekert Leibbrandt [b]

[a] *Department of Civil, Computational Science and Aeronautical Technologies Engineering, Roma Tre University, Rome, Italy*
[b] *Kopter Germany GmbH, Germany*

ARTICLE INFO

Communicated by Antonio Filippone

ABSTRACT

This paper presents the development of an algorithm for open-loop transfer functions identification and reduced-order modelling of a dynamical system, from closed-loop data with highly correlated inputs. Suitable for aeronautical applications (particularly for intrinsically unstable vehicles such as helicopters), it allows the identification of aircraft transfer functions from the knowledge of the time histories of arbitrary external inputs and the corresponding actuated controls and responses. After a numerical verification of the proposed approach considering a simple analytical aircraft dynamical system, it is successfully applied to a realistic engineering problem consisting of identifying the transfer functions of the AW-09 helicopter that relate pilot inputs to vehicle attitude and kinematics. It is shown that helicopter responses to arbitrary pilot inputs predicted by the reduced-order model representation of the helicopter dynamics based on the rational approximation of the identified transfer functions are in good agreement with those determined through the high-fidelity nonlinear flight dynamics solver used to evaluate the closed-loop database.

1. Introduction

Helicopter design and performance analysis are complex tasks that require the interaction of disciplines such as flight mechanics, structural analysis, aerodynamics, dynamics and control, aeroelasticity, power systems, avionics, and aeroacoustics. Due to this highly complex multiphysics interaction, complete and detailed helicopter simulation requires a significant computational effort, which is not always compatible with the designers' activity. By accepting a limited loss of precision and detail, it is possible to greatly reduce the computational effort required for simulation through the introduction of reduced-order models that describe the response of the entire helicopter or, depending on the specific needs, some of the physical phenomena involved (*i.e.*: the dynamics of the main rotor [1], the aerodynamic loads [2,3], or the wake inflow [4,5]). These yield simplified state-space representations of helicopter dynamics or physical phenomena involved, through which the system response is determined at a low computational cost [6,7].

Different approaches have been developed during the last decades to identify the reduced-order models of a given dynamic system. They can be generally divided into parametric and non-parametric methods. Parametric methods may identify the dynamics of a system in both the time and frequency domains and apply optimisation algorithms to evaluate the coefficients of a predefined reduced-order model [8]. If part of the involved physics phenomena can be suitably described a *priori*, it is possible to set preliminarily the value of some of the model coefficients, thus making the optimisation simpler. Non-parametric methods do not require initial assumptions about the form of the system governing equations, are applied in the frequency domain, and lead to a black-box model once the system dynamic is identified, [9]. Today, one of the most complete and advanced software for system identification in aeronautics is CIFER® [6,10]. It is a commercial code based on a comprehensive frequency-response approach widely used in the research community for system identification of full-scale and model-scale helicopters and aeroplanes [11–15]. Due to the poor stability of their dynamics, helicopters are often equipped with stability augmentation systems. Thus, it is impossible to identify the frequency response functions that relate the pilot input to vehicle responses through numerical or experimental data that do not include the controller action, and closed-loop data are the only available data.

This paper presents a novel methodology for reduced-order dynamic modelling of helicopters, based on the knowledge of closed-loop data with highly correlated inputs, which suitably combines different elements of the available dataset to obtain reliable and accurate identification of the open-loop transfer functions. It consists of a two-step process that begins with the identification of the open-loop transfer functions from closed-loop time domain responses provided by simulations or experiments, followed by their rational approximation [16] (similarly to [17] where the data set is obtained from flight tests). This

* Corresponding author.
E-mail address: m.gennaretti@uniroma3.it (M. Gennaretti).

https://doi.org/10.1016/j.ast.2024.109419
Received 24 May 2024; Received in revised form 21 July 2024; Accepted 21 July 2024
Available online 26 July 2024

Nomenclature

$\mathbf{A}, \mathbf{B}, \mathbf{C}$	Matrices of the Rational Approximation	$\mathbf{x}_{control}$	Vector of the control inputs from the controller
$\mathbf{F}(j\omega)$	Closed-loop transfer functions matrix	$\mathbf{x}_{pilot}$	Vector of the pilot inputs
$\mathbf{G}_{xx}(j\omega)$	Inputs auto-spectra matrix	$\mathbf{x}_{total}$	Vector of the total inputs
$\mathbf{G}_{yy}(j\omega)$	Outputs auto-spectra matrix	$\mathbf{y}$	Vector of the outputs
$\mathbf{G}_{xy}(j\omega)$	Input/Output cross-spectra matrix	γ	Scaling factor of non-linear terms
$\mathbf{H}(j\omega)$	Open-loop transfer functions matrix	γ^2_{xy}	Ordinary coherence
$\mathbf{K}(j\omega)$	Feedback controller transfer functions matrix	γ^2_{xym}	Multiple coherence
$k^p_{()}$	Coefficient of the controller proportional gain	(Φ, Θ, Ψ)	Euler angles
$k^i_{()}$	Coefficient of the controller integrative gain	$\theta_0, \theta_s, \theta_c$	Main rotor collective, longitudinal and lateral pitches
(p, q, r)	Angular velocities in the body frame	$\theta_{ail}, \theta_{rud}$	Airplane aileron and rudder angles
$\mathbf{r}$	Vector of the additional states from rational matrix approximation	θ_p	Tail rotor collective pitch
		θ_{pert}	Perturbations of the pilot inputs
(u, v, w)	Centre of mass velocity components in the body frame	ω	Frequency

system identification method is implemented in the in-house developed tool *Qopter*, which uses the z-transform of responses to chirp inputs to derive the transfer functions, while their rational approximation is obtained through a least square optimization scheme [16].

The present methodology is first validated by assessing its capability to identify the transfer functions of two simplified vehicles (an aeroplane and a helicopter) from outputs obtained through analytical representations of their controlled dynamics. Then, it is applied to a realistic problem of engineering interest regarding the controlled dynamics of the AW09 helicopter. The reduced-order helicopter model determined by exploiting a data set of responses obtained through high-fidelity simulations is validated by comparing the corresponding responses to arbitrary pilot inputs with those directly given by the high-fidelity flight-dynamics model.

Finally, note that the proposed algorithm, although developed for rotorcraft analysis and design purposes, is still general and can be conveniently used in all those applications where the identification of unstable systems from controlled closed-loop data is necessary (see, for example, [18] and [19]).

2. Transfer function identification and reduced-order modelling

The methodology proposed for the identification of reduced-order models of multi-input/multi-output (MIMO) systems, like a helicopter, from closed-loop data, consists of the following steps:

- evaluation of samples within a given frequency domain of the uncontrolled system transfer functions, extracted from time-domain, small-perturbation closed-loop (controlled) responses;
- rational approximation of the sampled transfer functions by application of a least-square technique.

This work focuses specifically on the first step of the identification procedure for the case where a MIMO data set from a controlled system is available instead of a set of single-input/multiple-output responses. Fig. 1 depicts the general scheme of a helicopter response problem when a stability augmentation system is included. The identification of the vehicle transfer functions is essential to perform flight dynamics analysis like the assessment of flying qualities, but it is a non-trivial task in this case. Indeed, in this case, due to the presence of a controller that stabilises the system, it is impossible to perform numerical simulations that provide the responses to a single input perturbation because the outputs are the result of combinations of multiple inputs (as dictated by the control law). Similarly, if the data come from flight tests, they are necessarily affected both by pilot action and stability augmentation system multi-input control action. Therefore, a technique capable of dealing with MIMO datasets must be introduced to identify the system transfer functions from available numerical or experimental responses.

For $\mathbf{F}(j\omega)$ and $\mathbf{H}(j\omega)$ which denote, respectively, the closed-loop and aircraft transfer matrices, and for $\mathbf{K}(j\omega)$ which denotes the matrix of the feedback controller, the following relationship can be analytically derived [20].

$$\mathbf{H}(j\omega) = \mathbf{F}(j\omega)[\mathbf{I} + \mathbf{K}(j\omega)\mathbf{F}(j\omega)]^{-1} \tag{1}$$

In this case, once the $\mathbf{F}$ matrix is identified, the $\mathbf{H}$ matrix is straightforwardly derived. However, the feedback control system may not be known and/or be too complex and may include strongly nonlinear terms. Thus, a more general and convenient way for determining the open-loop transfer functions consists of the application of the approach explained below, which is based on the availability of a suitable dataset of closed-loop system responses.

2.1. Aircraft transfer functions from uncorrelated noise-free database signals

Let us introduce, for the dynamic system representing a controlled helicopter, the vectors $\mathbf{y}$ and $\mathbf{x}$ which collect, respectively, the M outputs and the N inputs of the helicopter subsystem. Therefore, as indicated in Fig. 1, the N inputs are derived from the combination of pilot commands and controller feedback, that is, $\mathbf{x} = \mathbf{x}_{total} = \mathbf{x}_{pilot} - \mathbf{x}_{control}$.

Then, let us also assume that the available numerical or experimental input/output dataset consists of noise-free, small-perturbation time histories of all inputs and corresponding outputs, $\mathbf{x}^k(t)$ and $\mathbf{y}^k(t)$ with $k = 1, ..., \hat{N}$ (database composed of $\hat{N}$ elements). Hence, it is formally possible to define the following relation among their harmonic components

$$\tilde{\mathbf{y}}^k(j\omega) = \mathbf{H}(j\omega)\,\tilde{\mathbf{x}}^k(j\omega) \tag{2}$$

If $\hat{N} \geq N$ and at least N elements of the input/output database are linearly independent (uncorrelated), Equation (2) can be defined N times at a discrete number of points within a frequency range of interest, and for each point these linear relations can be combined in the following compact form

$$\mathbf{Y} = \mathbf{H}\,\mathbf{X} \tag{3}$$

with

$$\mathbf{Y} = \begin{bmatrix} \tilde{y}^1_1 & \dots & \tilde{y}^N_1 \\ \vdots & \ddots & \vdots \\ \tilde{y}^1_M & \dots & \tilde{y}^N_M \end{bmatrix}; \quad \mathbf{X} = \begin{bmatrix} \tilde{x}^1_1 & \dots & \tilde{x}^N_1 \\ \vdots & \ddots & \vdots \\ \tilde{x}^1_N & \dots & \tilde{x}^N_N \end{bmatrix} \tag{4}$$

where each column is derived from one of the $\hat{N}$ database elements and each row is an input/output channel. Thus, samples of the transfer functions at the discrete number of points considered within the frequency range of interest can be easily determined as

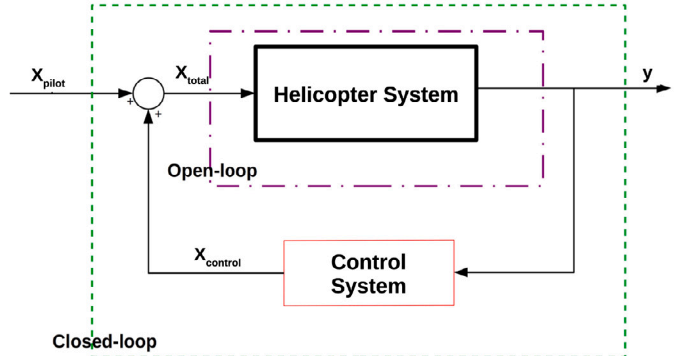

Fig. 1. Block diagram representation of helicopter dynamics.

$$\mathbf{H} = \mathbf{Y}\mathbf{X}^{-1} \tag{5}$$

and these values are the inputs for the application of the second and third steps of the process providing the reduced-order modelling of the helicopter transfer functions.

2.2. Aircraft transfer functions from correlated noisy database signals

Database signals may be generated by correlated inputs and/or affected by disturbances and measurement noise (in particular, those given by experimental measurements).

A general approach aimed at determining the frequency samples of the aircraft transfer functions requires the introduction of the following cross-spectra for each element of the database:

$$G^{ni}_{xx}(j\omega) = \frac{2}{T}|\tilde{x}^*_n(j\omega)\tilde{x}_i(j\omega)| \tag{6}$$

and

$$G^{im}_{xy}(j\omega) = \frac{2}{T}|\tilde{x}^*_i(j\omega)\tilde{y}_m(j\omega)| \tag{7}$$

where G^{ni}_{xx} denotes the cross-spectrum between the n-th and the i-th inputs, G^{im}_{xy} denotes the cross-spectrum between the i-th input and the m-th output, and T represents the signal observation time window. In fact, it is possible to show that for each element of the database, the frequency samples of the $[M \times N]$ transfer function matrix, $\hat{\mathbf{H}}(j\omega)$, can be evaluated through the following relation [21]

$$\hat{\mathbf{H}}^T = \mathbf{G}^{-1}_{xx}\mathbf{G}_{xy} \tag{8}$$

where $\mathbf{G}_{xx}$ and $\mathbf{G}_{xy}$ represent the matrices which collect the cross spectra in Equations (6) and (7).

However, effective application of this relation requires that the total inputs (combination of pilot commands and controller action, in flight dynamics problems) are not correlated or weakly correlated [22]. In our problem, where the multi-variable vectors $\mathbf{x}^k$ are affected by the control system feedback, considerable correlation among the total inputs typically occurs (see Fig. 1). To overcome this difficulty, in the proposed approach, the transfer functions are determined averaging the outputs of identification problems of the type of Equation (8) relating to several (at least 2) elements of the database. Specifically, if $\hat{\mathbf{G}}_{xx}$ and $\hat{\mathbf{G}}_{xy}$, respectively, represent the $[(N \times K) \times N]$ and the $[(N \times K) \times M]$ matrices obtained by sequentially ordering by column the matrices $\mathbf{G}^k_{xx}$ and $\mathbf{G}^k_{xy}$ determined for any k-th database element considered, namely

$$\hat{\mathbf{G}}_{xx} = \begin{bmatrix} \mathbf{G}^1_{xx} \\ \vdots \\ \mathbf{G}^k_{xx} \\ \vdots \\ \mathbf{G}^K_{xx} \end{bmatrix}; \quad \hat{\mathbf{G}}_{xy} = \begin{bmatrix} \mathbf{G}^1_{xy} \\ \vdots \\ \mathbf{G}^k_{xy} \\ \vdots \\ \mathbf{G}^K_{xy} \end{bmatrix} \tag{9}$$

the compact form of the identification problems of the type of that in Equation (8) repeated for all the considered K database elements is given by

$$\hat{\mathbf{G}}_{xx}\mathbf{H}^T = \hat{\mathbf{G}}_{xy} \tag{10}$$

where $\mathbf{H}$ denotes the $[M \times N]$ solution matrix of these problems.

Then, by introducing the Moore-Penrose pseudo-inverse of the matrix $\hat{\mathbf{G}}_{xx}$ which is given by

$$\hat{\mathbf{G}}^+_{xx} = (\hat{\mathbf{G}}^T_{xx}\hat{\mathbf{G}}_{xx})^{-1}\hat{\mathbf{G}}^T_{xx}$$

the transfer matrix is determined, for each frequency, by the following expression

$$\mathbf{H}^T = \hat{\mathbf{G}}^+_{xx}\hat{\mathbf{G}}_{xy} \tag{11}$$

This novel approach yields the transfer matrix as the least square approximation of the different solutions of Equation (8) written for each of the K database elements considered, which differ due to the noise affecting the signals.

It should be noted that, although this formulation is formally equivalent to that proposed by Bendat [21], it does not require that the inputs in each element of the database are linearly independent. Note also that the required value of K depends on the perturbations $\mathbf{x}_{pilot}$ considered in the available database: if, for instance, each element of the database derives from the perturbation of a single pilot command, the definition of a well-conditioned problem is ensured for $K = N$.

Finally, it is important to note that the quality of the results obtained by the proposed algorithm can be assessed by the evaluation of the coherence function, which is a measure of the linearity of the relationship between the outputs and inputs collected in the dataset. For instance, considering a single-input/single-output problem, the coherence is defined as follows (ordinary coherence)

$$\gamma^2_{xy} = \frac{|G_{xy}|^2}{G_{xx}G_{yy}} \tag{12}$$

In the case of a noiseless input, unit coherence means that the output is fully linearly dependent on the input. For MIMO systems, indications similar to those provided for SISO problems by the ordinary coherence are given by the multiple coherence which is defined as [23]

$$\gamma^2_{xy_m} = \frac{\mathbf{G}^T_{xy}\mathbf{G}^{-1}_{xx}\mathbf{G}_{xy}}{G_{yy}} \tag{13}$$

where G_{yy} is the auto-spectrum of the $\tilde{y}_m$ output. The closer this value is to unity, the more the output considered is linearly dependent on the set of inputs [23].

2.3. Reduced-order model

As indicated by the aforementioned two-step identification procedure, to determine the reduced-order model of the aircraft dynamics, the transfer matrix sampled in the range of frequency of interest is approximated in a rational-matrix form through the application of a least-square procedure [16]

$$\mathbf{H} \approx \mathbf{C}[s\mathbf{I} - \mathbf{A}]^{-1}\mathbf{B} \tag{14}$$

where $\mathbf{A}$, $\mathbf{B}$ and $\mathbf{C}$ are real, fully populated matrices, and s denotes the Laplace-domain variable. The matrix $\mathbf{A}$ is a $[P \times P]$ matrix containing the P poles of the rational expression, $\mathbf{B}$, is a $[P \times N]$ matrix, and $\mathbf{C}$ has dimensions $[M \times P]$.

Finally, combining the i/o relation $\tilde{\mathbf{y}} = \mathbf{H}\,\tilde{\mathbf{x}}$, with Equation (14) and transforming into time domain provides the following differential model that describes the helicopter dynamics, as derived from the transfer function matrix identified from the closed-loop dataset

$$\begin{cases} \mathbf{y} = \mathbf{C}\mathbf{r} \\ \dot{\mathbf{r}} = \mathbf{A}\mathbf{r} + \mathbf{B}\mathbf{x} \end{cases} \tag{15}$$

where $\mathbf{r}$ is the vector of the states introduced by the poles of the approximated transfer function matrix. The number of these states defines the order of the identified model.

3. Numerical investigation

The numerical investigation aims to validate the proposed algorithm for the identification of open-loop transfer functions and reduced-order modelling of vehicle dynamics based on knowledge of a database of closed-loop controlled responses to highly correlated command inputs, such as those obtainable from numerical simulations or in-flight data.

First, we consider two problems for which a simplified analytical representation of the dynamics of the vehicle is available. Specifically, the first case deals with the lateral-directional dynamics of an aeroplane, whereas the second one concerns the description of the dynamics of the mid-weight Bo-105 helicopter. The datasets of closed-loop controlled responses of the vehicles to input perturbations are determined by numerical time integration of known analytical models. The proposed identification algorithm is then applied, and the obtained open-loop transfer functions are compared with the analytical ones.

Next, we examine the problem of determining the computational tool for open loop transfer functions and reduced-order model of the AW-09 helicopter from a dataset of responses provided by a nonlinear, comprehensive computational tool for helicopter flight simulation.

3.1. Controlled lateral-directional dynamics of the LJ25-D aeroplane

This application of the proposed identification procedure is presented to prove its effectiveness when controlled MIMO system datasets with highly correlated inputs are available. To this purpose, we consider the stabilized lateral-directional dynamics of the LJ-25D aeroplane presented by Berger et al. in [14,24] which includes the action of a complex and realistic controller.

Following [24], a Simulink model of the aeroplane, including filters, sensors and actuators, is implemented and used to simulate the time responses to arbitrary pilot inputs. Once the time histories of outputs and control surface positions are collected, the proposed algorithm is applied to identify the open-loop transfer functions from closed-loop data. In particular, aileron deflections (α_a) and rudder deflections (α_r) are recorded and used as inputs, and a database of two elements is determined by numerical simulations: one set of inputs and controlled outputs is obtained by perturbing the pilot aileron control, and the second one is obtained by perturbing the pilot rudder control; both perturbations are done following a chirp-type signal as in Fig. 2.

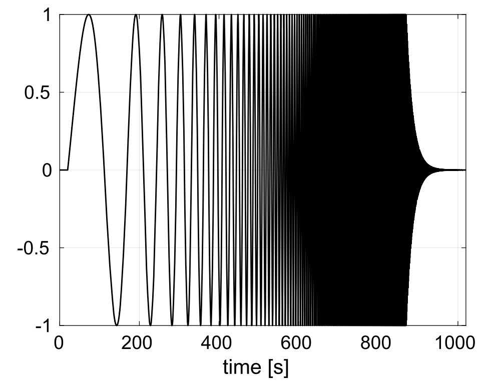

Fig. 2. Example of chirp-type signal used as input in the transfer function identification process.

Figs. 3 and 4 show the comparison between the transfer functions regarding roll angular velocity, p, and sideslip angle, β), given by the known analytic model, identified through the proposed procedure which combines both elements of the dataset (see Equation (11), MIMO-modified-AR in Figs. 3 and 4), and determined by the conventional approach that uses, separately, the responses triggered by aileron and rudder perturbations (respectively MIMO-A and MIMO-R in Figs. 3 and 4, see Equation (8)).

Note that the conventional approach is strongly affected by the cross-correlation between inputs. In [6] a threshold of the cross-correlation equal to 0.5 is indicated as a threshold above which the identified transfer functions are not sufficiently accurate since the contribution of each input to a given output cannot be distinguished. This issue is overcome by the proposed method, which combines data from different experiments to obtain the system's transfer functions. Fig. 5 shows the cross-correlation between the inputs in the two elements of the database considered for the lateral-directional dynamics of the LJ-25D aircraft. The red curve represents the cross-correlation between inputs of the first element of the database (MIMO-A). It has an average value equal to 0.8, which is well beyond the threshold value and, as expected, the transfer functions corresponding to the conventional approach (i.e., by Equation (8)) are quite inaccurate, as depicted in Figs. 3 and 4. Regarding the cross-correlation between the inputs of the second element of the database (MIMO-R), it has a low average value (0.5) in a frequency range $0 - 15$ rad/s, but is quite high at low frequencies. Consequently, the transfer functions identified by the conventional approach (MIMO-R) and depicted in Figs. 3 and 4 show a better accuracy than those obtained by MIMO-A, but still present significant discrepancies with respect to the analytical ones. Instead, although using the same database elements with significantly correlated inputs, Figs. 3 and 4 prove that the proposed approach (MIMO-modified-AR) provides very accurate transfer functions.

3.2. Bo-105 helicopter dynamics

This section examines the application of the proposed identification algorithm to an analytical representation of the dynamics of the Bo-105 mid-weight helicopter. The investigation focuses on the evaluation of the capability of the proposed methodology to extract the linearised open-loop rotorcraft model starting from the responses given by a controlled nonlinear representation of it. Specifically, considering the linearised representation of the Bo-105 given in [25] stabilised through a simple proportional-integrative (PI) controller acting on (p, q, r), the proposed approach is applied to an extended version of it obtained by arbitrarily adding nonlinearities to the system. It reads

$$\begin{aligned} \dot{\mathbf{y}} &= \mathbf{A}\mathbf{y} + \mathbf{f}(\mathbf{y}) + \mathbf{B}\mathbf{x} \\ \mathbf{x} &= \mathbf{x}_{pilot} + \mathbf{K}\mathbf{y} \end{aligned} \tag{16}$$

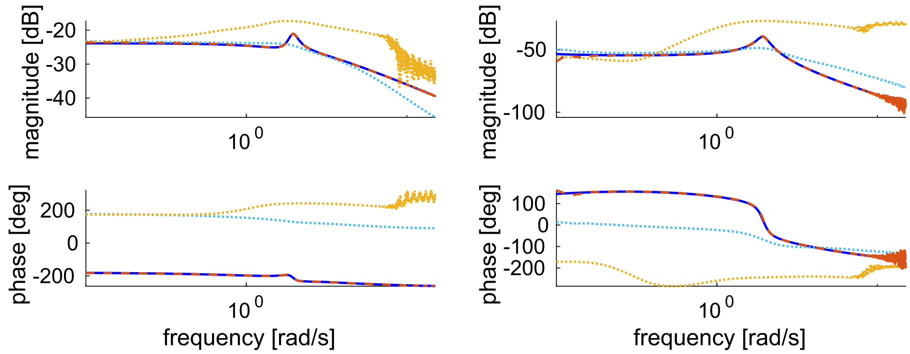

(a) p vs α_a (b) β vs α_a

Fig. 3. LJ25-D aeroplane transfer functions, aileron input. Solid line: analytical model; dotted cyan line: MIMO-A; dotted orange line: MIMO-R; dash-dotted line: MIMO-modified-AR.

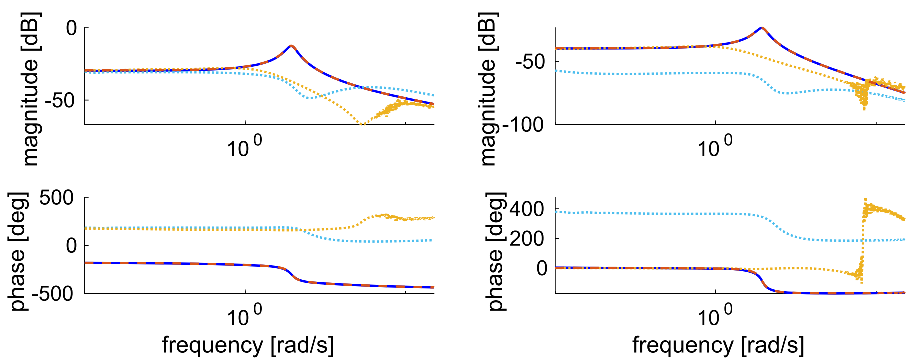

(a) p vs α_r (b) β vs α_r

Fig. 4. LJ25-D aeroplane transfer functions, rudder input. Solid line: analytical model; dotted cyan line: MIMO-A; dotted orange line: MIMO-R; dash-dotted line: MIMO-modified-AR.

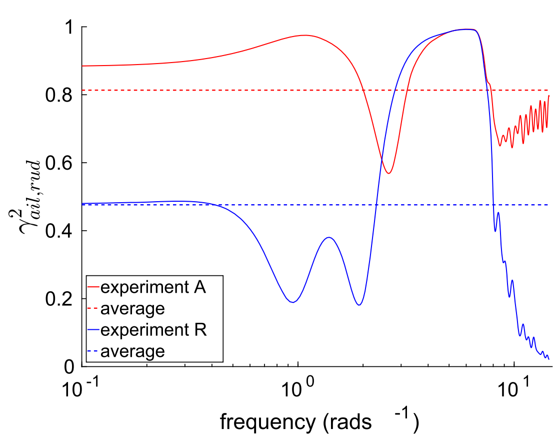

Fig. 5. Cross-correlation between control inputs.

where $\mathbf{y} = \{u, v, w, p, q, r, \Theta, \Phi\}^T$ collects the flight dynamics variables, the pilot inputs include collective pitch, cyclic pitch and pedal, $\mathbf{x}_{pilot} = \{\theta_0, \theta_s, \theta_c, \theta_p\}^T$, whereas $\mathbf{f}(\mathbf{y})$ denotes the nonlinear contributions which are defined as

$$f_i = \gamma \sum_j rand(0:1)_{ij}\, y_j \tag{17}$$

The nonlinear controlled helicopter model in Equation (16) is implemented in Matlab Simulink and the time responses to a set of chirp-type perturbations of the pilot inputs are evaluated. Several values of the input perturbation and scaling factor, γ, of nonlinear term are considered: $\gamma = 10^{-2}, 10^{-3}, 10^{-4}$ and $\theta_0 = \theta_s = \theta_c = \theta_p = \theta_{pert} = 0.25°, 0.5°$.

For some of the relevant longitudinal dynamics transfer functions, Figs. 6 to 9 show the comparisons between the uncontrolled linear analytical model given in [25] and two models identified by the proposed approach. These results show that as nonlinear terms and input perturbations decrease, the identified transfer functions tend to those of the analytical model, even though the process seems to identify somewhat more damped poles. In the presence of higher nonlinear terms and for greater input perturbations, the identification process captures the asymptotic behaviour of the transfer functions, whereas fails to correctly place poles and zeros of the systems. These observations are confirmed by the rest of the results obtained by the numerical investigation according to the variation of the parameters γ and θ_{pert}, which are not shown for the sake of conciseness.

Then, the identified transfer functions are collected in a matrix $\mathbf{H}$, approximated in the rational form of the type of Equation (14), and a time-domain reduced-order model of the helicopter is obtained by inverse transformation into the time domain.

For inputs consisting of step functions, Fig. 10 and Fig. 11 depict the corresponding kinematic responses of the uncontrolled helicopter determined by the analytical linear model given in [25] and by the reduced-order models based on the identified transfer functions presented in Figs. 6 to 9. These figures clearly show the presence of unstable poles in uncontrolled helicopter dynamics and show that small nonlinear disturbances do not significantly affect the proposed identification procedure (see dotted lines in Figs. 6 to 9). However, because of the

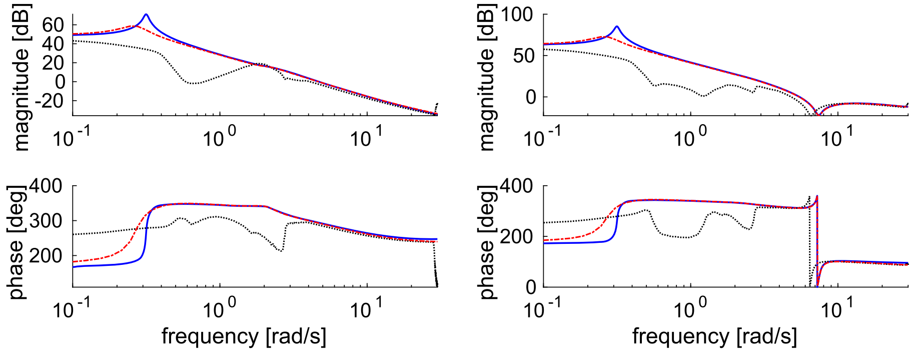

(a) u vs θ_0 (b) u vs θ_s

Fig. 6. Bo-105 helicopter transfer functions, u output. Solid line: analytical model [25]; dotted line: identified model for $\gamma = 10^{-3}, \theta_{pert} = 0.5°$; dot-dashed line: identified model for $\gamma = 10^{-4}, \theta_{pert} = 0.25°$.

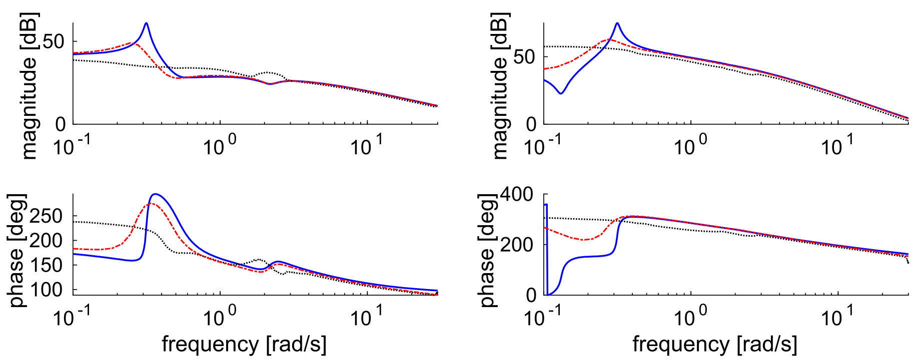

(a) w vs θ_0 (b) w vs θ_s

Fig. 7. Bo-105 helicopter transfer functions, w output. Solid line: analytical model [25]; dotted line: identified model for $\gamma = 10^{-3}, \theta_{pert} = 0.5°$; dot-dashed line: identified model for $\gamma = 10^{-4}, \theta_{pert} = 0.25°$.

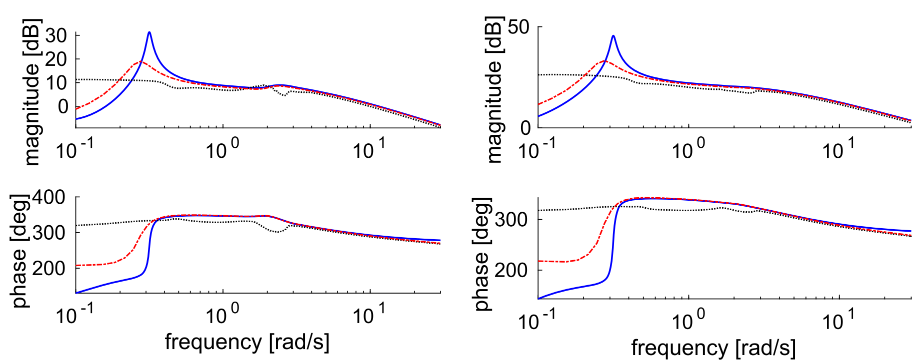

(a) q vs θ_0 (b) q vs θ_s

Fig. 8. Bo-105 helicopter transfer functions, q output. Solid line: analytical model [25]; dotted line: identified model for $\gamma = 10^{-3}, \theta_{pert} = 0.5°$; dot-dashed line: identified model for $\gamma = 10^{-4}, \theta_{pert} = 0.25°$.

instability of the uncontrolled system, the discrepancies increase with time.

In order to have an asymptotically decreasing response the reference and the identified helicopter models are combined with a proportional-integral feedback control law to stabilise helicopter dynamics. For the control gains assumed to be equal to $k^p_{\theta_C - p} = 0.01, k^p_{\theta_S - q} = 0.1, k^p_{\theta_P - r} = -0.4, k^i_{\theta_C - p} = -0.01, k^i_{\theta_S - q} = 1.0$ (where superscripts indicate if the gain is related to proportional or integral feedback), Fig. 12 shows the angular velocity responses to the same inputs considered in Fig. 11 and confirms the fidelity of the identified model.

3.3. Simulation of the AW09 helicopter dynamics

The proposed approach for aircraft transfer function identification is now applied to a more realistic problem regarding the flight dynamics of the AW09 helicopter. The main characteristics of this helicopter are

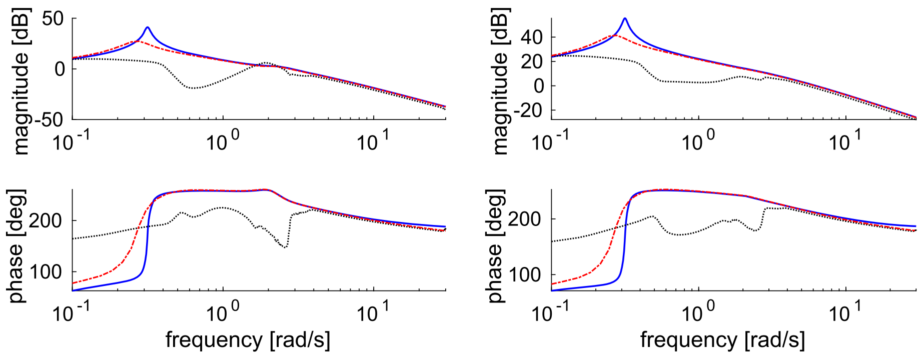

(a) Θ *vs* θ_0 (b) Θ *vs* θ_s

Fig. 9. Bo-105 helicopter transfer functions, Θ output. Solid line: analytical model [25]; dotted line: identified model for $\gamma = 10^{-3}, \theta_{pert} = 0.5°$; dot-dashed line: identified model for $\gamma = 10^{-4}, \theta_{pert} = 0.25°$.

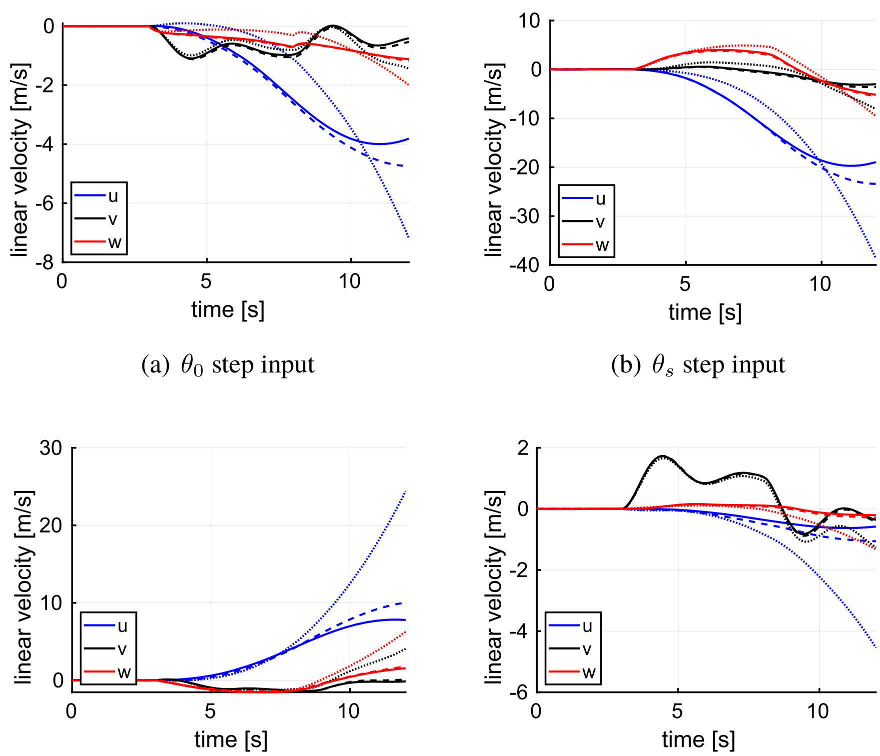

(a) θ_0 step input (b) θ_s step input

(c) θ_c step input (d) θ_p step input

Fig. 10. Uncontrolled Bo-105 helicopter velocity responses to pilot inputs. Solid line: analytical model in [25]; dashed line: identified reduced-order model for $\gamma = 10^{-4}$; dotted line: identified reduced-order model for $\gamma = 10^{-3}$.

Table 1
AW09 main characteristics.

mass	2500 kg
MR type	articulated
MR radius	5.5 m
MR number of blades	5
TR radius	0.6 m
TR number of blades	10

reported in Table 1. The linear reduced-order model to be identified is in the form of the standard helicopter dynamics representation which relates the four pilot control inputs (namely, collective, longitudinal and lateral cyclic pitch, and pedal, θ_0, θ_s, θ_c, θ_p) to the centre-of-mass velocities (u, v, w), angular velocities (p, q, r) in the body frame, and attitude angles (Φ, Θ, Ψ) [25].

The trim speed is 60 kn, and the dataset used for the identification of the open-loop transfer function matrix consists of a set of responses to chirp perturbations of the pilot inputs that are applied while keeping the stability augmentation system active. These responses are evaluated using a high-fidelity aeromechanic solver (see Sec. 3.3.1). Although one command at a time is perturbed, the controller produces perturbations to all commands and, hence, the response is generated by a full input vector, $\mathbf{x}_{total}$. The transfer functions are identified within the frequency range $0.2 \leq \omega \leq 8$ rad/s.

The reduced-order helicopter model obtained following the procedure described in Sec. 2 is then validated through comparison of the predicted responses to arbitrary inputs with those directly evaluated by

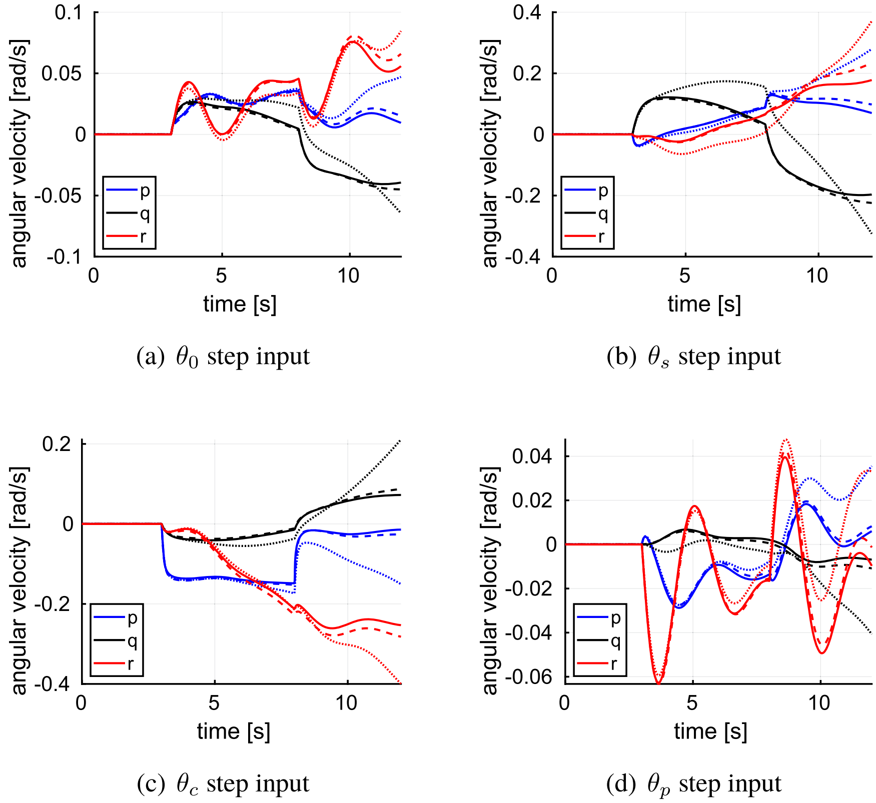

(a) θ_0 step input (b) θ_s step input

(c) θ_c step input (d) θ_p step input

Fig. 11. Uncontrolled Bo-105 helicopter angular velocity responses to pilot inputs. Solid line: analytical model in [25]; dashed line: identified reduced-order model for $\gamma = 10^{-4}$; dotted line: identified reduced-order model for $\gamma = 10^{-3}$.

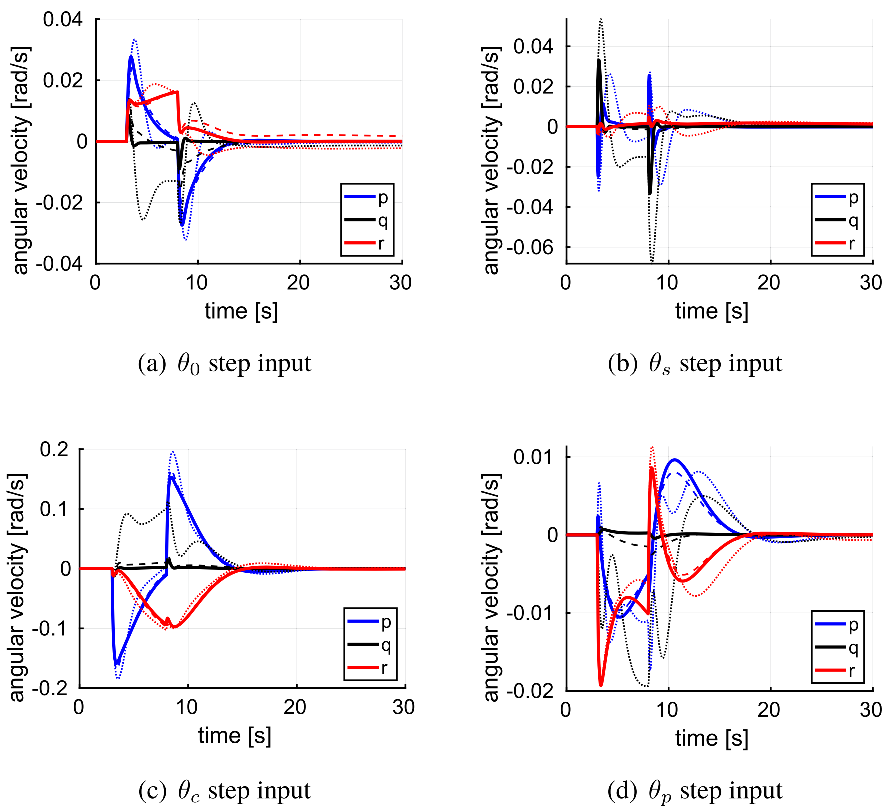

(a) θ_0 step input (b) θ_s step input

(c) θ_c step input (d) θ_p step input

Fig. 12. Controlled Bo-105 helicopter angular velocity responses to pilot inputs. Solid line: analytical model in [25]; dashed line: identified reduced-order model for $\gamma = 10^{-4}$; dotted line: identified reduced-order model for $\gamma = 10^{-3}$.

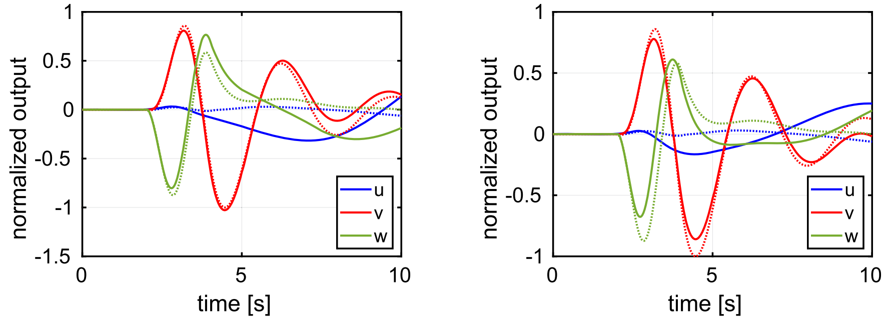

(a) $A = 0.5^\circ$ (b) $A = 1.0^\circ$

Fig. 13. Uncontrolled AW09 helicopter responses to θ_0 input. Solid line: identified reduced-order model; dashed line: FlightLab.

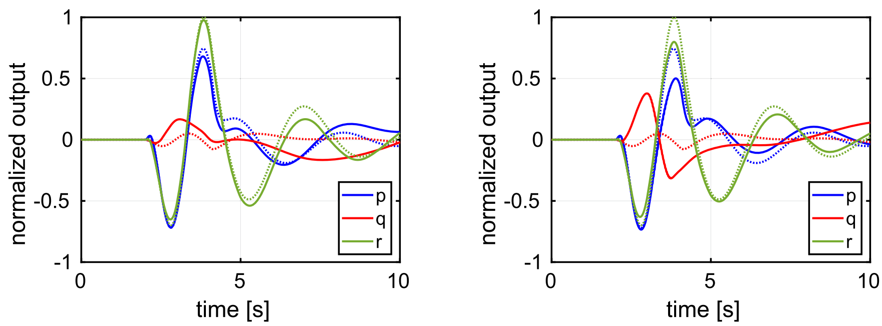

(a) $A = 0.5^\circ$ (b) $A = 1.0^\circ$

Fig. 14. Uncontrolled AW09 helicopter responses to θ_0 input. Solid line: identified reduced-order model; dashed line: FlightLab.

the high-fidelity aeromechanic solver (see Sec. 3.3.1). The predictions concern both uncontrolled and controlled helicopter flight and are given in terms of the model kinematic output. The arbitrary input applied for the simulations is the following single-harmonic, windowed signal

$$y(t) = A\sin(\omega t)[H(t) - H(t - 2\pi/\omega)] \quad (18)$$

where H is the Heaviside function, $\omega = 1.3$ rad/s and two different amplitudes ($A = 0.5^\circ$ and $A = 1.0^\circ$) are used to assess the accuracy of the linearized helicopter model identified as a function of the input amplitude.

3.3.1. High-fidelity aeromechanic solver

The dataset used for model identification is obtained by FlightLab simulations [26]. The computational model consists of a fully coupled, nonlinear, aeromechanic solver. The aerodynamic modelling is based on a quasi-steady strip-theory approach, with Pitt-Peters dynamic wake inflow model. The aerodynamic coefficients (lift, drag, and pitching moment) are derived from sectional look-up tables. The structural degrees of freedom include the six fuselage rigid body motion DOFs, and the multi-blade flap and lag angles. The structural DOFs of the tail rotor blades are not included in the model, as it is intended for flight dynamics purposes.

The body motion observed by the inertial frame is described through the components of the centre of mass velocity and the angular velocity expressed in a body frame.

The model features a conventional control system with collective, lateral, and longitudinal cyclic and pedal control. The main rotor swashplate routine computes the feathering angle, rate, and acceleration for each blade, starting from azimuth and rotor speed. The motion of each blade is imposed on the feathering hinges. Two flight configurations are considered, one with and one without feedback control. The model with feedback control includes rate controllers for p, q and r, using three independent proportional and integral (PI) feedback controllers on the lateral cyclic, longitudinal cyclic, and pedal channels; feedback control is not considered for the collective pitch.

3.3.2. Response of uncontrolled helicopter

The validation of the reduced-order open-loop helicopter model identified from closed-loop data begins with the analysis of the time response of the uncontrolled rotorcraft to arbitrary pilot inputs.

A single pilot command is perturbed in each test. Two different amplitudes of the pilot inputs are considered, as mentioned above (see Equation (18)). The predictions provided by the reduced-order model are compared with those directly obtained by the high-fidelity computational tool, given in terms of data normalized to the maximum value of the examined set of curves (thus, the range of all graphs is $[-1 : 1]$). For the sake of conciseness, only the results which are most representative of the overall quality of the reduced-order model are presented. Specifically, Figs. 13 and 14 depict the helicopter response to collective in terms of linear and angular velocities, respectively. Fig. 15 shows the angular velocities generated by the lateral cyclic input. These results demonstrate satisfactory agreement between the predictions obtained by the identified model and those determined by the high-fidelity computational tool, particularly (as expected) for outputs with the greatest amplitude and when the smallest input is considered.

3.3.3. Responses of controlled helicopter

Next, the response of the reduced-order helicopter model combined with a controller is examined. The same pilot inputs considered for the uncontrolled helicopter case are applied, and two sets of control gains are introduced. The first set of gains coincides with that considered for the evaluation of the database (see above) and is referred to as normal gains, whereas the second set of gains is ten times smaller than the first one (referred to as low gain). Similarly to the investigation concerning the uncontrolled helicopter, the predictions given by the reduced-order

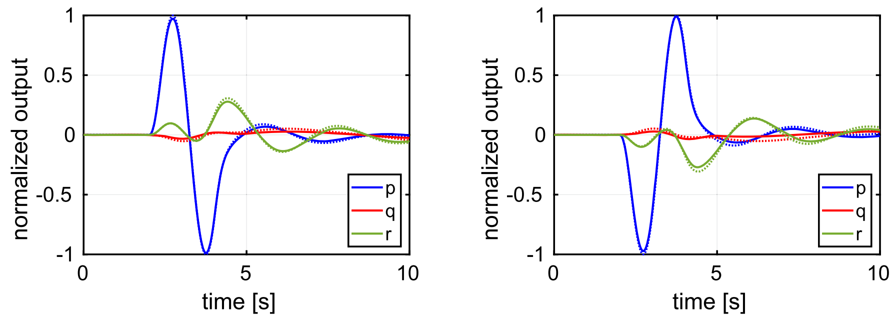

(a) $A = 0.5°$ (b) $A = 1.0°$

Fig. 15. Uncontrolled W09 helicopter responses to θ_c input. Solid line: identified reduced-order model; dashed line: FlightLab.

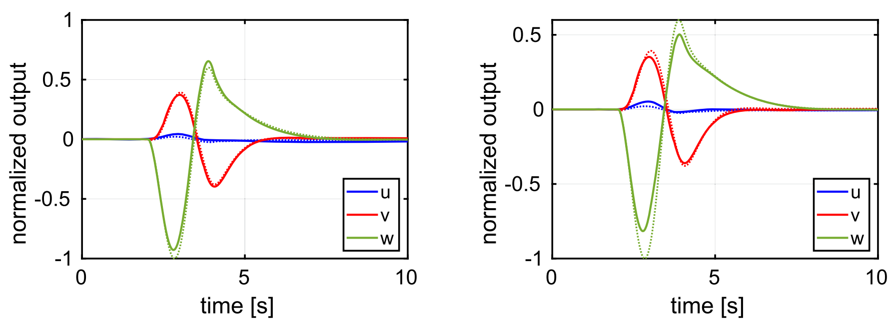

(a) $A = 0.5°$ (b) $A = 1.0°$

Fig. 16. Normal-gain, controlled AW09 helicopter responses to θ_0 input. Solid line: identified reduced-order model; dashed line: FlightLab.

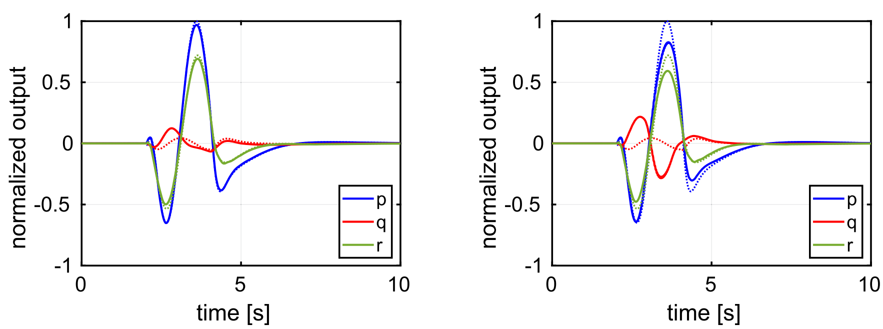

(a) $A = 0.5°$ (b) $A = 1.0°$

Fig. 17. Normal-gain, controlled AW09 helicopter responses to θ_0 input. Solid line: identified reduced-order model; dashed line: FlightLab.

helicopter model combined with the controller are compared with those obtained by FlightLab simulations.

Normal Gain. The kinematic outputs obtained for the controlled helicopter when normal gains are applied are presented in Figs. 16 to 18. These figures show that the presence of the controller produces a clear improvement of the agreement between the results given by the application of the reduced-order helicopter model and those provided by FlightLab. In particular, the agreement is very good when the smallest pilot inputs are considered, whereas some discrepancies arise for larger pilot inputs (however, this operating condition has to be considered as an out-of-design application of the proposed, linear, model).

These results prove that the proposed reduced-order helicopter model can be effectively applied to the design of reliable control laws, thus replacing more complex high-fidelity computational tools.

Low Gain. The predicted helicopter responses with low-gain control actuation are presented in Fig. 19-21.

The objective of this analysis is to assess the reliability of the identified reduced-order helicopter model by testing its prediction capability in the presence of a significantly different controller than the one applied for the determination of the database used in the identification process.

Overall, the predictions based on the reduced-order model are confirmed to be in good agreement with FlightLab simulations, particularly when related to the smallest pilot inputs. It is worth noting that, as expected, the predictions relating to reduced values of gains yield less damped (although stabilized) helicopter outputs, which present a more wavy behaviour than in the normal-gain control case (see, for instance, Figs. 16 and 19).

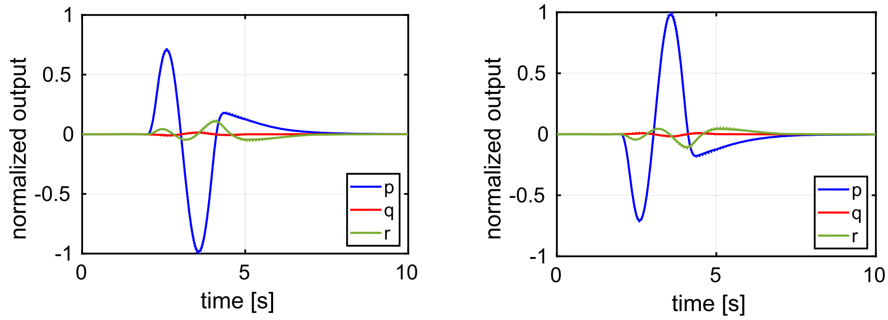

(a) $A = 0.5°$ (b) $A = 1.0°$

Fig. 18. Normal-gain, controlled AW09 helicopter responses to θ_c input. Solid line: identified reduced-order model; dashed line: FlightLab.

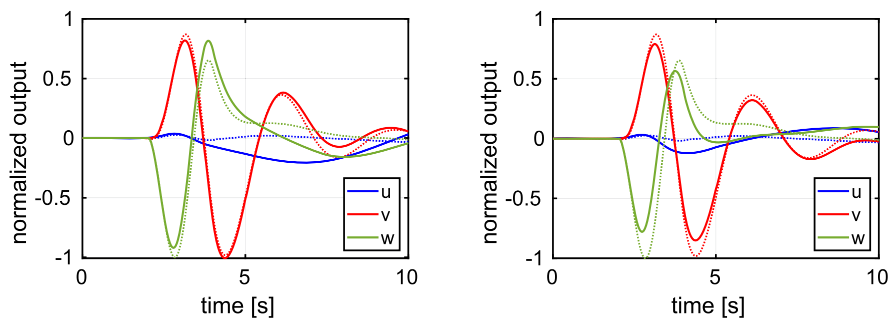

(a) $A = 0.5°$ (b) $A = 1.0°$

Fig. 19. Low-gain, controlled AW09 helicopter responses to θ_0 input. Solid line: identified reduced-order model; dashed line: FlightLab.

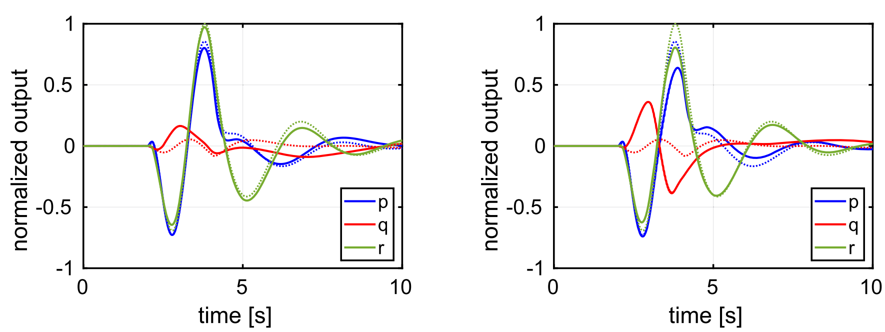

(a) $A = 0.5°$ (b) $A = 1.0°$

Fig. 20. Low-gain, controlled AW09 helicopter responses to θ_0 input. Solid line: identified reduced-order model; dashed line: FlightLab.

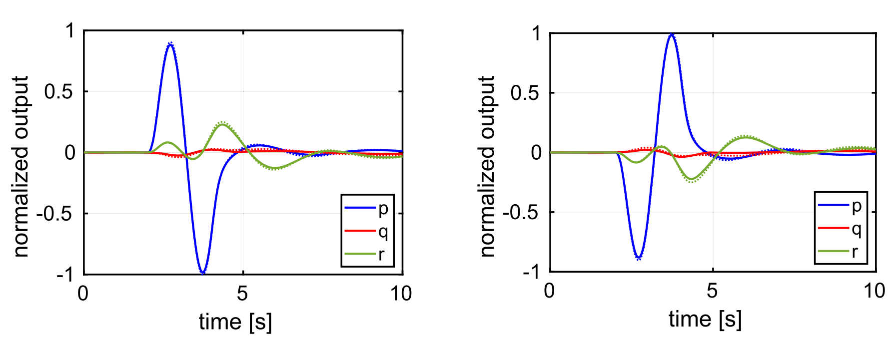

(a) $A = 0.5°$ (b) $A = 1.0°$

Fig. 21. Low-gain, controlled AW09 helicopter responses to θ_c input. Solid line: identified reduced-order model; dashed line: FlightLab.

4. Conclusions

A novel methodology for the identification of an open-loop, reduced-order model of a dynamical system based on the knowledge of closed-loop, highly-correlated, data has been developed and applied to different test cases with an increasing level of complexity. It is particularly suitable for unstable systems for which the database that can be used to identify the open-loop transfer functions is necessarily related to controlled responses, and hence produced by highly-correlated inputs. Two different types of numerical investigations have been presented to validate the proposed methodology. First, it is applied to two simplified analytical aircraft dynamics models: the lateral-directional dynamics model of the LJ25-D aircraft combined with a realistic controller, and the Bo-105 helicopter flight dynamics model including the stability augmentation system. In these cases, the identified open-loop transfer functions have been successfully compared with analytical ones, thus demonstrating the capability of the proposed method to successfully overcome the problem of highly correlated inputs in system identification. Since nonlinear artificial terms were included in the helicopter model, the obtained results have also proven the capability of the proposed identification algorithm to extract the linear part of the system dynamics. As expected, the identification accuracy decreases as the input perturbations used to determine the closed-loop database and/or the relevance of the nonlinear terms increase. Then, the proposed methodology has been applied to identify the transfer functions of the AW09 helicopter and the corresponding reduced-order model, exploiting a database of controlled responses to pilot commands obtained by the high-fidelity FlightLab computational tool. The accuracy of the identified AW09 model has been assessed by comparing its predictions of vehicle kinematics due to arbitrary pilot inputs with those provided directly by FlightLab. Some responses have been examined for both the uncontrolled (unstable) and controlled helicopters. Although the agreement between the results given by the identified reduced-order model and FlightLab is quite good in the case of an uncontrolled vehicle, it presents some small discrepancies due to the difficulty in capturing the exact placement of the unstable poles. The correlation becomes of excellent quality when the helicopter is controlled (particularly, when a high value of proportional gain is used). The comparison with FlightLab simulations proves that the helicopter reduced-order model identified from a database of controlled responses provides accurate flight dynamics simulations and, in particular, is capable of providing a reliable estimation of the effects produced by the actuation of an arbitrary controller. Summarising the outcomes of the validation analysis, the algorithm can successfully identify the open-loop transfer function from closed-loop data also in the case of highly-correlated inputs but it begins to fail in prediction accuracy when the non-linear content of the model and/or the input perturbations used to determine the closed-loop database increase. In particular, the presence of a relevant non-linear content directly impacts the evaluation of the system's poles, and hence it should be care of the user to verify with some time-domain validation signals the accuracy of the obtained reduced-order model. Future improvements will follow two lines of research: (i) the inclusion of a grey-box scheme to make use of prior knowledge of the system dynamics and characteristic parameters (like, for instance, mass parameters, flight velocity, relationship between degrees of freedom), and (ii) the extension to nonlinear identification in order to overcome the weak points highlighted in this work and develop more general dynamic models.

CRediT authorship contribution statement

Claudio Pasquali: Conceptualization, Methodology, Software, Validation, Writing – original draft, Writing – review & editing. **Jacopo Serafini:** Conceptualization, Methodology, Validation, Writing – original draft, Writing – review & editing. **Massimo Gennaretti:** Conceptualization, Methodology, Supervision, Writing – review & editing. **Riekert Leibbrandt:** Software, Validation, Writing – original draft.

Declaration of competing interest

The authors declare that they have no known competing financial interests or personal relationships that could have appeared to influence the work reported in this paper.

Data availability

No data was used for the research described in the article.

Acknowledgements

This research was performed within the Roma Tre University participation in the CORAL project financed by Kopter Germany (GmbH), a member of the Leonardo Group.

References

[1] R. Gori, F. Pausilli, M.D. Pavel, M. Gennaretti, State-Space Rotor Aeroelastic Modeling for Real-Time Helicopter Flight Simulation, Advanced Materials Research, vol. 1016, Trans Tech Publ, 2014, pp. 451–459.
[2] M. Gennaretti, D. Muro, Multiblade reduced-order aerodynamics for state-space aeroelastic modeling of rotors, J. Aircr. 49 (2) (2012) 495–502, https://doi.org/10.2514/1.C031422.
[3] C. Pasquali, N. Spyropoulos, R. Leibbrandt, M. Gennaretti, V. Riziotis, S. Radler, G. Bernardini, G. Papadakis, Rotor aeroelastic stability assessment in the new CORAL framework, in: 49th European Rotorcraft Forum (ERF), Bückeburg, DE, 2023.
[4] M. Gennaretti, C. Pasquali, F. Cardito, J. Serafini, G. Bernardini, R. Celi, Dynamic wake inflow modeling in ground effect for flight dynamics applications, in: AHS 73rd Annual Forum & Technology Display, 2017.
[5] C. Pasquali, M. Gennaretti, G. Bernardini, J. Serafini, State-space dynamic inflow modelling for hovering rotors in fixed- and moving-ground effect, Aerosp. Sci. Technol. 140 (2023) 108414, https://doi.org/10.1016/j.ast.2023.108414.
[6] C.R. Theodore, M.B. Tischler, J.D. Colbourne, Rapid frequency-domain modeling methods for unmanned aerial vehicle flight control applications, J. Aircr. 41 (4) (2004) 735–743, https://doi.org/10.2514/1.4671.
[7] M.B. Tischler, M.G. Cauffman, Frequency-response method for rotorcraft system identification: flight applications to BO 105 coupled rotor/fuselage dynamics, J. Am. Helicopter Soc. 37 (3) (1992) 3–17, https://doi.org/10.4050/JAHS.37.3.3.
[8] H. Unbehauen, G. Rao, A review of identification in continuous-time systems, Annu. Rev. Control 22 (1998) 145–171.
[9] P.E. Wellstead, Non-parametric methods of system identification, Automatica 17 (1) (1981) 55–69, https://doi.org/10.1016/0005-1098(81)90084-4.
[10] CIFER, CIFER® | comprehensive identification from FrEquency responses, https://www.sjsu.edu/researchfoundation/resources/flight-control/cifer.php, 2000.
[11] M.B. Tischler, C.A. Tumashofski, Flight test identification of SH-2G flapped-rotor helicopter flight mechanics models, J. Am. Helicopter Soc. 47 (1) (2002) 18–32, https://doi.org/10.4050/JAHS.47.18.
[12] B. Mettler, T. Kanade, M.B. Tischler, System identification modeling of a model-scale helicopter, Tech. Rep., Carnegie Mellon University, The Robotics Institute, 2000.
[13] Grip Håvard Fjær, Wayne Johnson, Carlos Malpica, Daniel P. Scharf, Milan Mandić, Larry Young, Brian Allan, Bérénice Mettler, Martin Miguel San, Johnny Lam, Modeling and identification of hover flight dynamics for NASA's Mars helicopter, J. Guid. Control Dyn. 43 (2) (2020) 179–194, https://doi.org/10.2514/1.G004228.
[14] T. Berger, M.B. Tischler, M.E. Knapp, M.J. Lopez, Identification of multi-input systems in the presence of highly correlated inputs, J. Guid. Control Dyn. 41 (10) (2018) 2247–2257, https://doi.org/10.2514/1.G003530.
[15] T. Berger, E.L. Tobias, M.B. Tischler, O. Juhasz, Advances and modern applications of frequency-domain aircraft and rotorcraft system identification, J. Aircr. (2023) 1–23, https://doi.org/10.2514/1.C037275.
[16] R. Gori, J. Serafini, M. Molica Colella, M. Gennaretti, Assessment of a state-space aeroelastic rotor model for rotorcraft flight dynamics, CEAS Aeronaut. J. 7 (3) (2016) 405–418, https://doi.org/10.1007/s13272-016-0196-1.
[17] A. Kuppusamy, S.J. Yoon, Experimental flight testing and system identification of eurocopter AS365N2 dauphin helicopter using CIFER®, Int. J. Appl. Eng. Res. 12 (24) (2017) 14287–14298.
[18] H.-J. Ahn, S.-W. Lee, S.-H. Lee, D.-C. Han, Frequency domain control-relevant identification of mimo amb rigid rotor, Automatica 39 (2) (2003) 299–307, https://doi.org/10.1115/GT2003-38597.
[19] R. Mandloi, P. Shah, Methods for closed loop system identification in industry, J. Chem. Pharm. Res. 7 (1) (2015) 892–896.
[20] D.S. Miller, Open loop system identification of a micro quadrotor helicopter from closed loop data, Master's thesis, University of Maryland, College Park, 2011.
[21] J.S. Bendat, A.G. Piersol, Random Data Analysis and Measurement Procedures, IOP Publishing, 2000.
[22] M.B. Tischler, R.K. Remple, Aircraft and Rotorcraft System Identification, American Institute of Aeronautics and Astronautics, Reston, VA, 2012.

[23] R.K. Otnes, Applied Time Series Analysis, vol. 1, Wiley-Interscience, 1978.
[24] T. Berger, M. Tischler, S.G. Hagerott, D. Gangsaas, N. Saeed, Lateral/directional control law design and handling qualities optimization for a business jet flight control system, in: AIAA Atmospheric Flight Mechanics (AFM) Conference, 2013, p. 4506.
[25] G.D. Padfield, Helicopter Flight Dynamics, Blackwell Science Ltd, 1996.
[26] R. Du Val, C. He, Flightlab modeling for real-time simulation applications, Int. J. Model. Simul. Sci. Comput. 8 (04) (2017) 1743003, https://doi.org/10.1142/S1793962317430036.